

## Research Article

# Simulation Analysis of 4G/5G OFDM Systems by Optimal Wavelets with BPSK Modulator

**Bullarao Domathoti** <sup>1</sup>, **Chengaiyah Ch** <sup>2</sup>, **SrinivasaRao Madala** <sup>3</sup>,  
**Afework Aemro Berhanu** <sup>4</sup> and **Yamarthi Narasimha Rao** <sup>5</sup>

<sup>1</sup>Department of Computer Science & Engineering, Shree Institute of Technological Education, Tirupati, 517501 A P, India

<sup>2</sup>Department of Electrical & Electronics Engineering, Sri Venkateswara University College of Engineering, Sri Venkateswara University, Tirupati 517501, India

<sup>3</sup>Department of Computer Science & Engineering, PACE Institute of Technology and Science, Ongole, India

<sup>4</sup>Department of Environmental Engineering, College of Biological and Chemical Engineering, Addis Ababa Science and Technology University, Addis Ababa, Ethiopia

<sup>5</sup>Department of CSE, School of Computer Science and Engineering, VIT-AP University, Amaravati -522237, Andhra Pradesh, India

Correspondence should be addressed to Bullarao Domathoti; [bullaraodomathoti@gmail.com](mailto:bullaraodomathoti@gmail.com) and Afework Aemro Berhanu; [afework.aemro@aastu.edu.et](mailto:afework.aemro@aastu.edu.et)

Received 24 March 2022; Revised 1 July 2022; Accepted 13 September 2022; Published 29 September 2022

Academic Editor: Rabeh Abbassi

Copyright © 2022 Bullarao Domathoti et al. This is an open access article distributed under the Creative Commons Attribution License, which permits unrestricted use, distribution, and reproduction in any medium, provided the original work is properly cited.

LTE (Long-Term Evolution) is one of the appropriate technologies to sever the requirement of the IoT (Internet of Things) together with mobile UE (User Equipment), because of priority services, high data rate, low latency, etc. LTE has received OFDM for the transmission because it meets the necessity of LTE-like range flexibility and empowers the cost gainful responses for the wide carriers. LTE offers big-data values, allows spectrum reframing, reduces cost, etc. We proposed a 4G/5G adopted OFDM based on the multi-equalizer and BPSK (Binary-Phase Shift Keying). The BER (Bit Error Rate) of the system is reduced through the optimal wavelet coefficient at the transmitter side. This optimal wavelet coefficient is obtained by applying a DWT (Discrete Wavelet Transform) to the input signal through a BFF (Binary Firefly) algorithm. The serial to parallel process is carried out through the BPSK modulation. At last, the multi-equalizer like MMSE (Minimized Mean Square Error) and MLE (Maximum Likelihood) is applied to the OFDM model to reduce the BER. The system is analyzed using the parameter like SER (Symbol Error Rate), spectral efficiency, MSE (Mean Square Error), and BER. The proposed methodology provides a better outcome than the other existing approaches.

## 1. Introduction

Smart IoT devices function as an important part of our lives unless any direct human intrusions. LTE is acting as a powerful technological solution for the broadband wireless approach networks and fast-improving data traffic needs from UEs and IoT devices because of its high data rate assist and another key characteristic. But, finding a small signal at additive white Gaussian noise (AWGN) from a small compression rating without signal reproduction is an enigmatic object [1]. Substantial recognition of the signal and authori-

zation of modulation as a moderate part of the signal were given further attention as a defamation measure. Different approvals have been proposed step by step [2]. OFDM (orthogonal frequency division multiplexing) signals are examined as a procedure of numerous sovereign random signals [3]. The applications of remote signals are GBS-denied, and areas are taken as of late, owing to the practically universal immediacy in many structures [4]. To utilize a directional antenna, we use a hypothetical route to the transmitter we got the orientation signal legitimately as of the transmitter [5]. Here, the transfers are used to get the signal

transmitted by the basis hub. The studies on the exhibition of hand-off helped OWC (RAOWC) display that it can widen strained transmitter the inclusion of strength and improve the heartiness of outlook imparting longer-extend distorting channels.

The information of transmission pace is extended normally using higher recurrence carriers, and microwave and millimeter-wave signals are taken as an example [6]. By figuring flex and progress, wavelet transform can multi-scale improve the signal. In the time area change, the signal to the wavelet space with the final goat that the vast majority of the signal vitality collected in barely any wavelet coefficients taken as an estimate [[7, 8]]. This wavelet coefficient is playing an important role in the domain of information which can able to process by using short-extend radio innovation that is considered an additional component for worms to increase with no web association. To control the malevolent signals in WSN and to shield it from infections and maggots, we need a solid security component [9]. The major problem in several frameworks is signal detection whereas the measurable signal handling technique is mostly utilized for the signal detection process [10]. The problem in the signal improvement is normally defined as the forecast problem which predicts the clean signal from the noise signal [11]. The major threats to the remote sensor are LTE signaling attacks whereas in the MIMO-OFDM framework, the signal discovery problem is observed as a component acknowledgment problem that is not included in the plan of conventional signal recognition [[12, 13]]. These issues are rectified by transmitting the neural signal obtained from the embedded cathodes to the outside unit [14].

## 2. Related Works

In 2017, Hassani et al. [15] had proposed Multitask Wireless Sensor Network (MWSN) for joining the LCMV Beamforming, DOA Assessment, and disseminated hub-Specific Signal Amplification. The low-position guess of the ideal signal was integrated with the grid based on the disseminated signal estimation method. Moreover, diverse signal preparing and undertaking were identified with the help of appropriated algorithm which helps to reduce the similar assets. Thereafter, the presented algorithm was utilized in the remote acoustic sensor organize circumstance along with numerous sources and it was efficient for the hypothetical results.

In 2016, de la Hucha Arce et al. [16] have presented a generalization for the utility of sensor signal. Here, a greedy method was utilized to track the bit that is assigned to the sensor. In addition to that, comparison of computational cost with available LMMSE (Linear Minimum Mean Squared Error) estimator is carried out.

In 2014, Chi and Li [17] have presented a waveform strategy based on the OFDM (Orthogonal Frequency Division Multiplexing) signal to eradicate the resolution conflict in medical ultrasound imaging. This method reduces the range side-lobe level of the signal to -96 dB and the peak side-lobe level is reduced to -80 dB.

In 2016, Zheng and Kostamovaara [18] have examined the statistical properties of ADC through AWGN (additive

Gaussian noise) input. Digitization is achieved through a 2-level comparator rather than the multi-bit ADC when there is a large average.

In 2016, Hwang et al. [19] had presented an SDR (Software-Defined Radio) method to establish the cross-platform LTE VSA (Long-term Evolution Vector Signal Analyzer). This method does not utilize the costly off-the-shelf VAS and it is separated into SA (Signal Acquisition) hardware as well as PC-based CS (Core Software). Here, the CS represents the SA control function and the process of the received LTE signal.

In 2014, Jerjawi et al. [20] have analyzed the LTE SC-FDMA (Long-term Evolution Single Carrier-Frequency Division Multiple Access) signals and the second-order cyclostationarity of the LTE SC-FDMA. Here, the investigation was carried out through the cyclostationarity-based detection algorithm, whereas the outcome obtained from the cyclic autocorrelation function is applied to the signal detection. The presented algorithm yields better performance for various channel constraints.

In 2015, Hwang et al. [19] have presented an ASI (Automatic Signal Identification) algorithm for recognizing the LTE and GSM signals. This algorithm is based on the pilot-induced second-order cyclostationarity. It provides a low signal-to-noise ratio without the channel estimation as well as the frequency and time synchronization process [T. [21]].

## 3. Proposed Approach: 4G/5G OFDM Systems Analysis

By utilizing the DWT method to the transmitter side of the OFDM system, the input signal's BER (Bit Error Rate) value can be lessened. Meta heuristics algorithms are utilized to enhance the DWT coefficients such as Haar, Daubechies, and Symlet. For the serial to parallel progression, improved coefficients and the BPSK are utilized, whereas, on the receiver side, the AWGN (adaptive white Gaussian noise) channel gets demodulated and decomposed transform technique is employed to the signals. The effectiveness of the presented approach is validated through the performance metrics such as BER, MSE, SER, and spectral efficiency.

### 3.1. OFDM System

- (a) OFDM is considered a fine-tuning and multiplexing. Usually, multiplexing indicates the self-governing signal of several systems
- (b) In an OFDM system, a multiplexing process is employed for the received signals and these signals are considered the sub-set of one essential signal
- (c) In the autonomous channel, signal is the first segment and later it is multiplexed to generate the OFDM bearer

3.2. *LTE with OFDM Model.* MIMO – OFDM system is incorporated with the 4G, 5G broadband because of the advancement in MIMO like it can transfer the different signals

through several antennas, whereas the OFDM channel splits the channel radio into the closely spaced sub-channels to deliver the signals at high speed. The LTE-OFDM structure is shown in Figure 1.

**3.3. LTE-OFDM Transmitter.** A transmitter includes the sub-carrier mapping, modulator-baseband, backward Fourier change, parallel-serial transformation, CP (cyclic prefix), and a computerized to-simple converter which are adopted by the DPSK modulator.

**3.4. LTE-OFDM Receiver.** OFDM collector includes a parallel-to-serial converter, analog to digital converter, RF segment, Fourier change, equalizer, CP remover, identifier, and sub-bearer de-mapper. The utilization of modulation types is based on the noise signal ratio of the received signal. The modulation signals are mapped to the subcarrier and its transfer through an IFFT. These modulations are also utilized to store control data of every subcarrier.

**3.4.1. DWT in the Input Signal.** The input signal is declined within time recurrence and that is depicted through DWT. The extraction processes of the transform wavelet are carried out through two steps. First, the signals are decomposed based on the distinct recurrence sub-groups. Second, the split-up signal of a specific recurrence sub-group is evaluated under numerous constraints. For  $s(t)$  signal, the variation in wavelet with  $\delta m, n(t)$  wavelet is given as follows

$$D(m, n) = \int_{-\infty}^{\infty} s(t) \cdot \delta m, n(t) dt. \quad (1)$$

The input signal is passed through the channels like high pass and low pass then the signals are separated by the wavelet filters into two sub-band called high-pass sub-band and low-pass sub-band. These sub-bands are again classified into two units and this process is repeated till an appropriate stage. The outcome of the low-pass channel is referred to as the estimated coefficient whereas DWT is used to eradicate the attribute from the various signals. There are numerous elective wavelets; some of the wavelet utilized in the presented work are given below.

- (1) Haar Wavelet
- (2) Daubechies Wavelet
- (3) Symlet Wavelet

(1) (1) *Haar Wavelet Transform Coefficient.* The two-dimensional Hor bandwidth is taken into account to carry out a filtering step, because it reduces the BER and computational duration, whereas  $m_t$  is expressed as follows.

$$m_t = H_t \omega_t, \quad (2)$$

where  $t$  represents the info signal and  $\omega_t$  denotes the Haar wavelet transform.

In the initial stage, the AA1 is decomposed, and this process is continued. Every stage of the wavelet includes two

advanced channels and a downsampler which is depicted in Figure 2.  $HP[t]$  is a discrete mother wavelet and it is referred to as a high-pass channel whereas,  $LP[t]$  is referred to as a low-pass channel and  $\downarrow 2$  represents the subsampling. In the initial stage, the AA1 is decomposed, and this process is continued. The mean estimation of the detail coefficient is defined by making the detail coefficient as normal.

$$d[c_t] = \sum c_t, \quad (3)$$

where  $\Delta_{c_t}$  represents the incentive means of estimation coefficient.

The standard deviation of the detail coefficient is evaluated through the square foundation of the mean worth.

$$\sigma_{c_t} = \sqrt{d[c_t] - (d[c_t])^2}, \quad (4)$$

where  $\sigma_{c_t}$  represents the standard deviation of estimation coefficient.

(2) (2) *Daubechies Wavelet Transform Coefficient.* The variation in the Daubechies wavelet is defined comparably through the Haar wavelet variation. The basic qualification between the wavelets incorporates the representation of scaling signal and wavelets. In the variation of the Daubechies wavelet, the scaling signal and wavelet have long backing which means it generates a contrast as well as midpoint and that utilizes a few more qualities from the signal. For each wavelet group, the orthogonal multiresolution generated by the balancing task  $\omega(t)$  is examined as follows.

$$\omega(t) = \sum_{n=0}^{N-1} c_n \omega(2x - n), \quad (5)$$

where  $(c_0, c_1, \dots \dots c_{N-1})$  a group of genuine numbers is referred to as scaling cover or succession.

(3) (3) *Symlet Wavelet Transform Coefficient.* It is one of the members of the dB frequencies family and is proposed by Daubechies. It compares the features of two wavelet members. It is referred a "sym" and later it is denoted through the quantity of evaporating minutes.

**3.4.2. Optimal Coefficients Selection Using BFF.** Firefly algorithm was proposed by Yang in the year 2007. This algorithm is inspired by the behavior and the flashing pattern of the fireflies. This algorithm is a metaheuristic population-based approach. The short and rhythmic flashes generated by the firefly are observed, whereas the pattern of the male and female fireflies is varied for each other. Fireflies communicate through bioluminescence which is a glimmering design [22]. FF contain certain benchmarks and they are as follows:

- (i) Fireflies are unisex; therefore, the attraction process does not depend on firefly sex
- (ii) The attractiveness of the fireflies is directly proportional to the brightness of the fireflies so if the

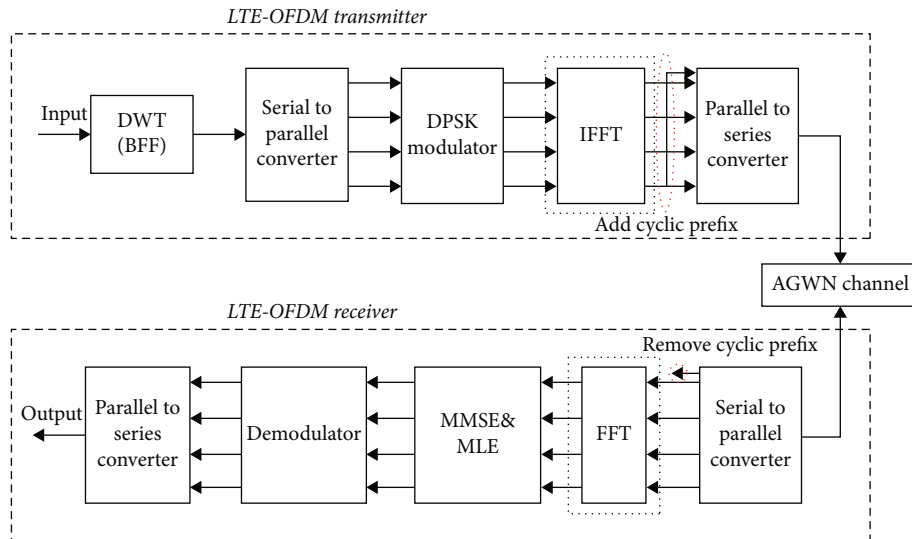


FIGURE 1: Structure of LTE-OFDM.

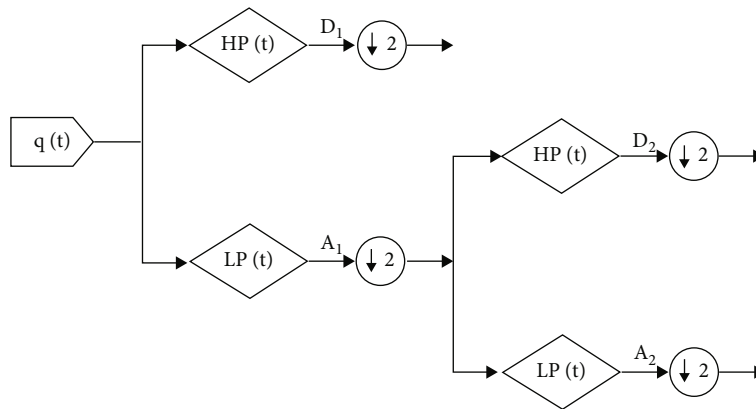
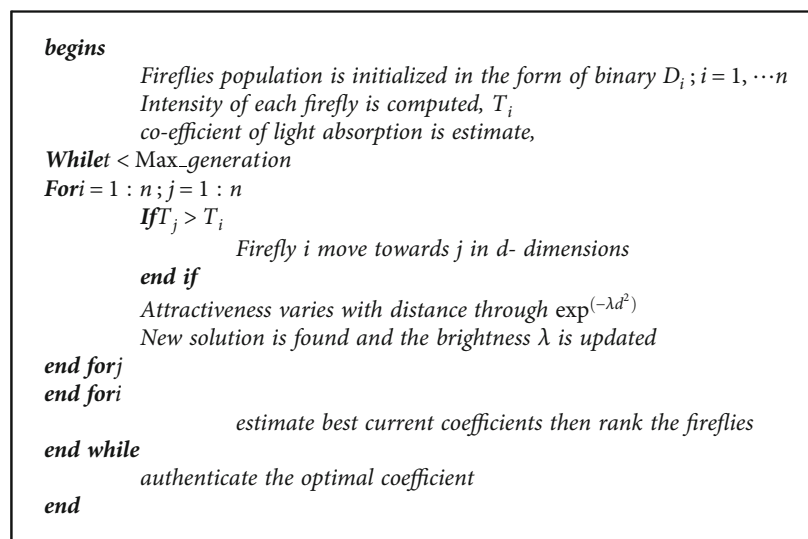


FIGURE 2: DWT decomposition.



ALGORITHM 1: BFF Algorithm

attractiveness and brightness decrease, then the distance between the flies is increased [23]. The flies with less brightness attract the flies with more brightness. If the firefly did not get the brighter one, then it moves randomly

- (iii) The landscape of the objective function is used to define the fireflies' brightness

(1) *Binary Firefly*. The firefly algorithm is handled through the binary structure. The consequence of this activity ranges from 0 and 1. After the application of the binarization technique, the appropriate 0 or 1 is obtained.

*Step 1.* Firefly population is initialized that is the coefficient of DWT  $D_i = D_1, \dots, D_n$  is initialized, where  $D_i = 1, \dots, n$ ; here,  $n$  specifies the absolute number of the coefficient. Here, the values are transferred in the form of binary and the choices are revised to generate a firefly swarm with the required size. The length of firefly space is equal to the absolute coefficient. The firefly population measures resolve the optimal coefficients.

*Step 2.* The light force intensity of the firefly is measured in this phase. Here, the wavelet coefficient is evaluated through the fitness function.

*Step 3.* The estimation of target role in each FF is recognized through the light intensity of the compared FF. The firefly with fewer magnificence is pulled in and the light intensity is expressed as

$$T_i = T_{i0} e^{-\lambda r^2}, \quad (6)$$

where  $T_{i0}$  represents the attractiveness with  $r = 0$  and  $\lambda$  represents the coefficient of absorption, which controls the light force reduction.

*Step 4.* Every firefly includes an engagement which are used for the enhancement of the firefly constraint.

$$\tau = \tau_0 e^{-\lambda r^2}, \quad (7)$$

where  $\tau_0$  indicates the quality of engaging at  $\text{attr} = 0$ .

The separation of fireflies  $a$  and  $b$  at positions  $a_p$  and  $b_q$  are characterized as follows:

$$r_{ab} = \sqrt{\sum_{f=1}^d (a_p^f - b_q^f)^2}, \quad (8)$$

where  $a_p^f$  indicates the  $f^{\text{th}}$  spatial coordinate's segment and  $d$  indicates the quantity measurements. At last, the progress of a firefly  $a$  is forced to the alternative in an attractive manner

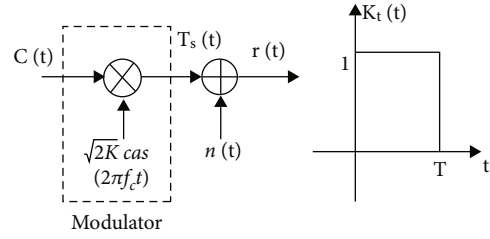


FIGURE 3: BPSK modulator.

and it is indicated as

$$A_p^{f+1} = A_p^f + \tau (A_b^f - A_a^f) + \sigma \left( \text{rand} - \frac{1}{2} \right), \quad (9)$$

where  $A_a^{f+1}$  indicates the situation of firefly in the next generation.

$A_p^f$  indicates the present situation of firefly  $A_a$ .

$\tau(A_b^f - A_a^f)$  represents the engaging quality.

$\sigma(\text{rand} - 1/2)$  indicates the random parameter  $\sigma$  and rand.

*Step 5.* The above process is continued until the optimal coefficient is obtained.

The BER of the input signal is reduced by selecting the optimal coefficient; after that, the input is transmitted to the LTE-OFDM transmitter. Then, the signals that are processed through the transmitter are explained in the further section.

*3.5. BPSK Modulation Technique.* BPSK is a two-phase balanced scheme in which two varied phase states in the transmitting signal are indicated through the zero's and one's in the double message. Figure 3 depicts the structure of BPSK modulation and Figure 4 illustrates the BPSK demodulation structure. The carrier is expressed as follows,

$$B(t) = P \cos(2\pi f_c t), \quad (10)$$

where  $P$  indicates the  $1\Omega$  load resistor's sinusoidal carrier peak estimation, whereas the power dispersed is expressed as follows,

$$R = 1/2P^2. \quad (11)$$

In the binary adjustment, two signals with antipodal produce the base error probability through the additional parallel signal arrangement. The probability of the error is reduced by allowing multiple waveforms to broadcast the data. The transmitting signal is characterized through  $K(t)$  and it is expressed as follows

$$K_T(t) = \begin{cases} 1 & 0 \leq t \leq T \\ 0 & \text{otherwise} \end{cases}. \quad (12)$$

$$c(t) = \sum_{l=-\infty}^{\infty} c_l K_T(t - lT); c_l \in \{+1, -1\}, \quad (13)$$

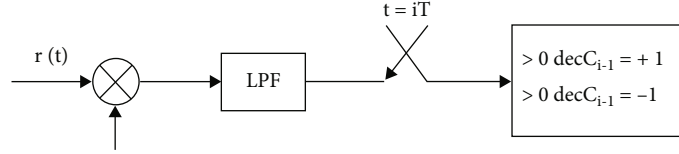


FIGURE 4: BPSK demodulator.

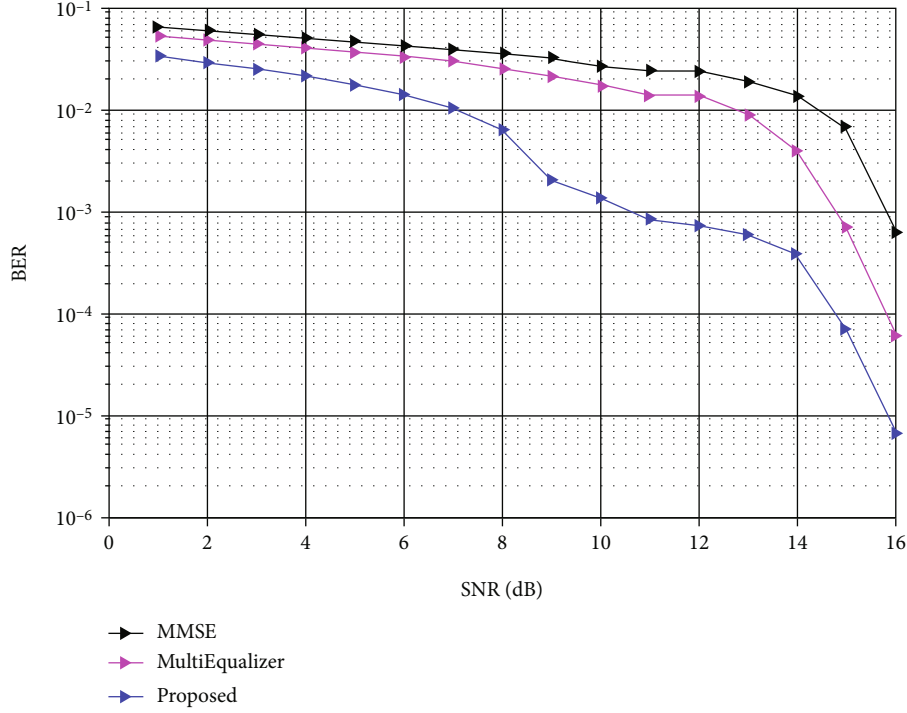


FIGURE 5: Comparison of 4G/5G OFDM with OFF methods based on BER.

where  $c(t)$  indicates the waveform information which includes an interminable succession of pulses with time  $T$  and height 1.

The signal that are transmitted are represented as,

$$T_s(t) = \sqrt{2K} \sum_{l=-\infty}^{\infty} c_l \cos(2\pi f_c t) K_T(t - lT), \quad (14)$$

$$T_s(t) = \sqrt{2K} \cos(2\pi f_c t + \varphi(t)),$$

where  $\varphi(t)$  indicates the waveform stage and  $K$  represents the signal force.

The energy of each transmitted piece is given as follows:

$$E = KT. \quad (15)$$

The AGWN presence provides the optimum recipient for BPSK, whereas the LPF (low-pass channel) is integrated with the baseband signal that is transmitted. The reaction is denoted as  $j(t) = K_T(t)$ . The yield of low-pass channel is given as follows

$$Y(t) = \int_{-\infty}^{\infty} \sqrt{\frac{2}{T}} \cos(2\pi f_c \tau) h(t - \tau) r(\tau) d\tau. \quad (16)$$

The capacity of the BPSK signal's data transfer is decreased through the separation process, whereas in the off-state, the capacity of the data transfer is reduced to  $1/T$ . After the modulation process, the input taken from the source encoder is grouped into a  $\log_2 M$  bits cluster by the S/P (Serial to Parallel) converter, where  $M$  indicates the digital modulation plan size which is utilized by every subcarrier. Here,  $n$  number of  $O_m$  symbols is generated. After that, the signals are plotted to the IFFT container [26] and these IFFT bins are relays on the symmetrical sub-transporters of the OFDM signal. Therefore, the communication of OFDM is expressed as follows:

$$O(l) = \frac{1}{l} \sum_{k=0}^{l-1} O(k) \exp\left(\frac{j2\pi kl}{L}\right). \quad (17)$$

By using the  $N$ -point FFT function, the unique signal of the recipient is reduced and it is expressed as follows:

$$Y(k) = \sum_{n=0}^{l-1} y(n) \exp\left(\frac{-j2\pi kn}{L}\right) + Z(k), \quad (18)$$

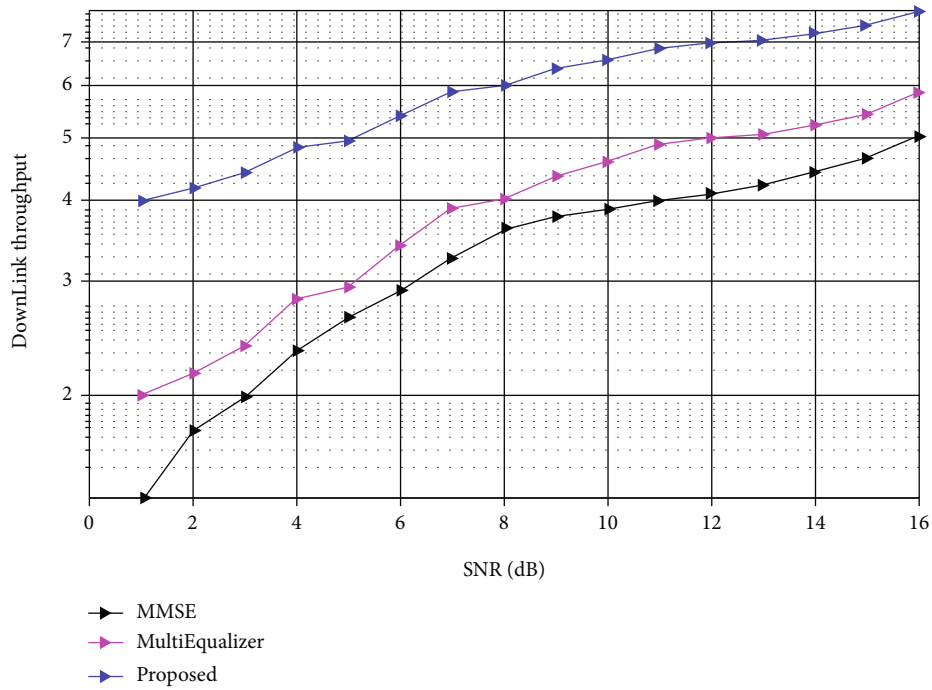


FIGURE 6: Comparison of 4G/5G OFDM with existing methods through DLT.

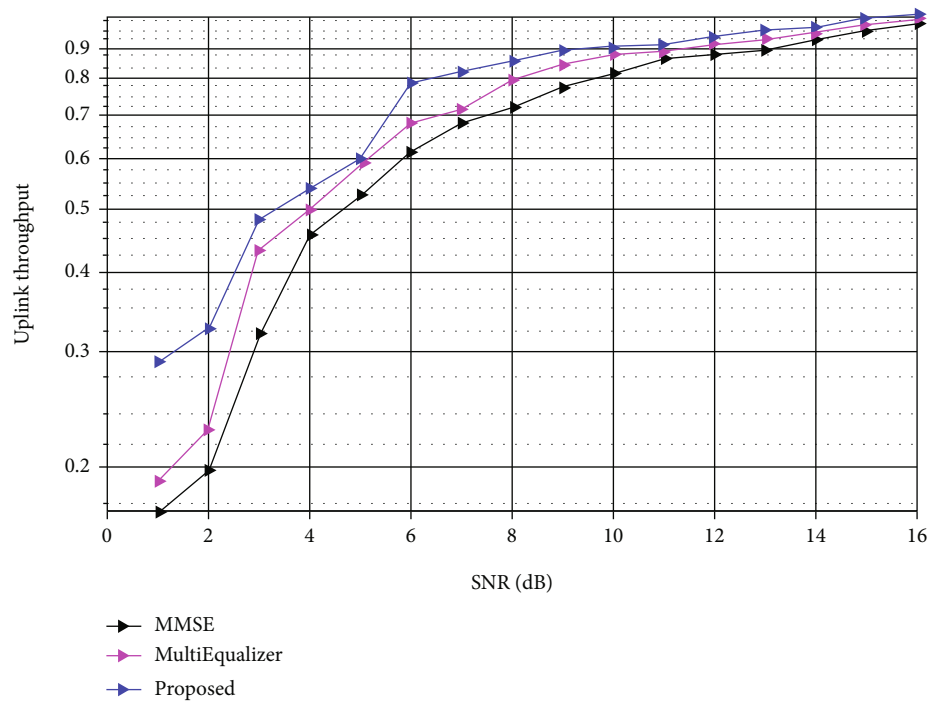


FIGURE 7: Comparative analysis of 4G/5G OFDM with OFF approach through ULT.

where  $Z(k)$  is the AWGN that exists in the channel and compares to the  $F(k)$  samples of FFT.

3.6. *AGWN Channel.* In the process of channel acknowledgment, the AGWN channel is a widely utilized numerical model. Here, the main source for the troubling impacts at the recipient

side is taken as warm commotion. The white Gaussian clamor is added by the AWGN channel to the signal. This is expressed as follows:

$$r_s(t) = T_s(t) + G(t), \tag{19}$$

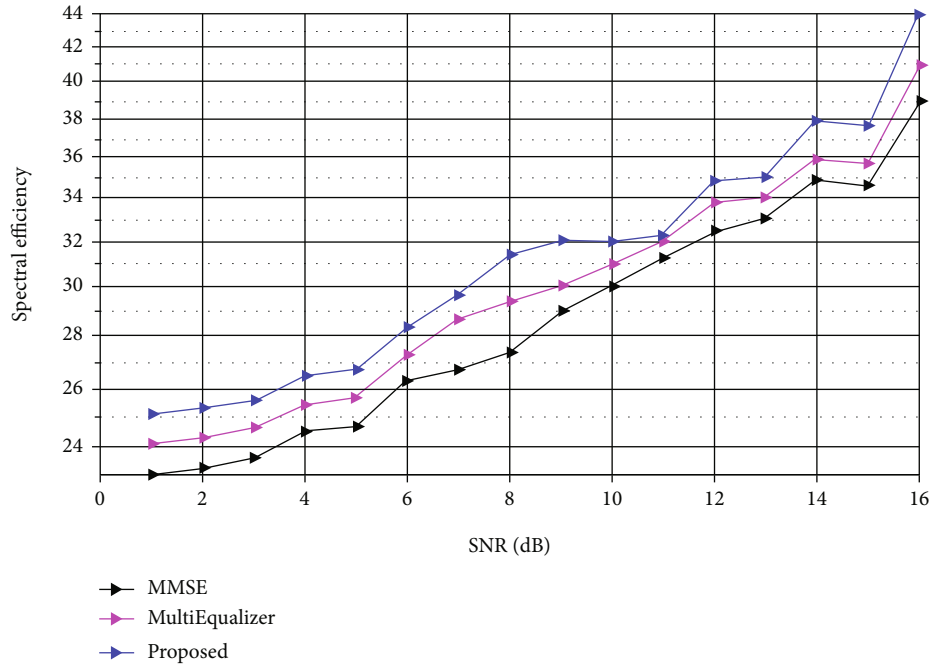


FIGURE 8: Comparative analysis of 4G/5G OFDM with existing method in terms of spectral efficiency.

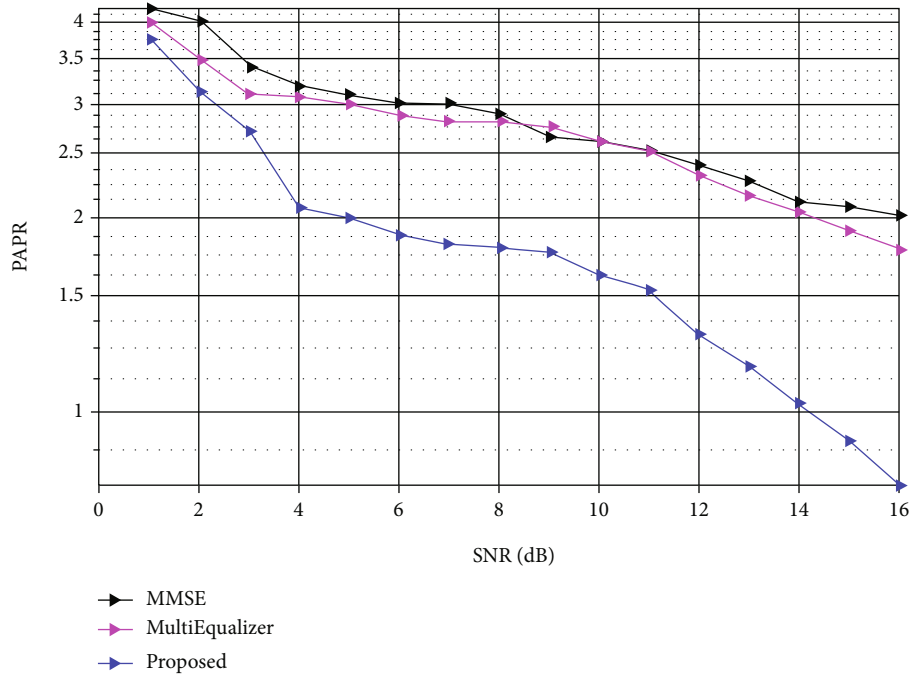


FIGURE 9: Comparison of 4G/5G OFDM with existing method in terms PAPR.

where  $r_s(t)$  and  $T_s(t)$  represent received and transmitted signal whereas  $G(t)$  indicates the white Gaussian noise that is added to the AWGN channel. Moreover, Gaussian approximation is employed for the noise test, and its function of thickness  $P_d(x)$  with fluctuation  $\sigma^2$  is given as follows

$$P_d(x) = \frac{1}{\sqrt{2\pi\sigma^2}} e^{-\frac{(x-m)^2}{2\sigma^2}}. \quad (20)$$

For example, the negative impacts of the multipath are reduced through transmitting the signal with shortest path to the multipath channel with high data rate.

**3.7. Multi-Equalizers for BER Reduction.** The traditional OFDM recipient normally supports the inverse procedure of transmission. Here, the OFDM recipient utilized the multi-equalizer to



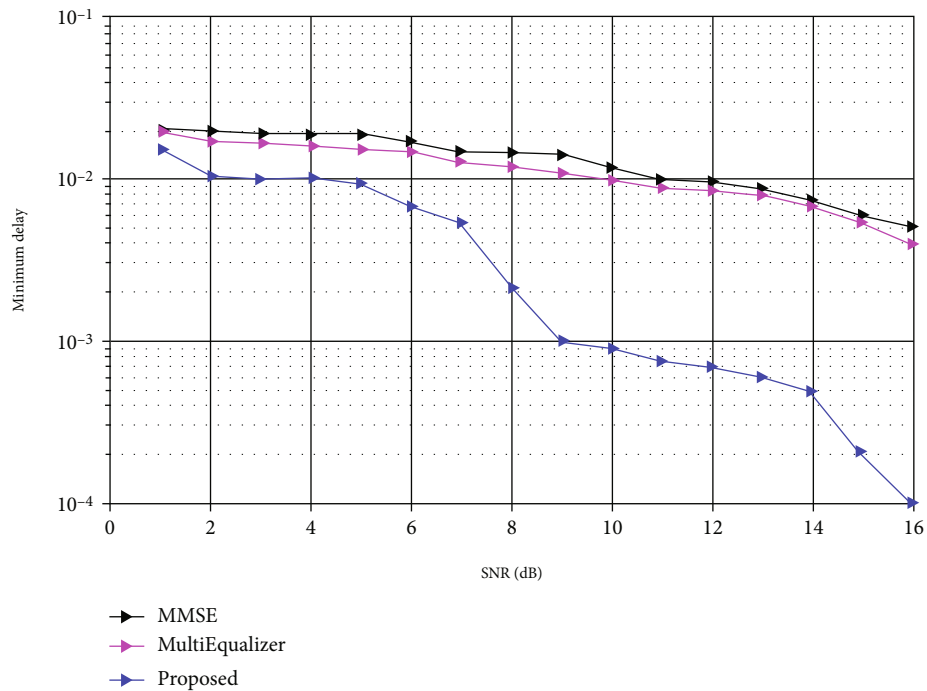


FIGURE 10: Comparative analysis of MSD for 4G/5G OFDM with existing method.

retrieve the signals which enhance the attributes of BER and retain better SNR.

**3.7.1. MMSE (Minimum Mean Square Error) Equalizer.** The MMSE arrangement includes various coefficients in which numerous coefficients are located for each example time to limit the error between the balanced and perfect signals. The MMSE recipient is utilized to diminish the average estimation error that occurs in the transmitted symbol. The capacity of the error estimation is communicated using the constraint (21).

$$e[t] = g[t] \otimes h[t], \quad (21)$$

where  $e[t]$  indicates the blunder at test time  $t$ , and  $g$  and  $h$  represent the column and segment vector of measurement, respectively, whereas  $g$  reserves the coefficient of the equation and  $h$  limits the received test.  $t$  denotes the cycles in the equalizer or time count.

**3.7.2. MLE (Maximum Likelihood Equalizer).** The MLE is more supreme than BER and is known as an elective approach when the PMF or PDF are recognized in the circumstance. This approach compares every signal that is received for selecting the probability. The MLE is expressed as follows

$$\text{MLE} = \text{argmin} \|h(y) - Vx\|^2, \quad (22)$$

where  $h(y)$  indicates the input signal. Here, the recipient diverges the vector and potential arrangement of the received signal whereas the ML equalizer evaluates the channel impulse response. The performance of the system is improved by periodically recognizing the signal rather than expanding the mul-

tifaceted nature. The MMSE-ML noise equalization reduces the BER of the LTE-OFDM signal.

## 4. Experimental Results

This research work is implemented in the MATLAB platform version 2015A with system configuration of i5 processors containing 4GB RAM. The main objective of the work is to reduce the BER (Bit Error Rate) through 4G/5G adopted OFDM. This reduction is carried out by selecting optimal wavelet coefficients through BFF (Binary Firefly) algorithm. Here, some other performance metrics like up and downlink throughput, minimum delay, and SNR are taken into account for the performance evaluation. The outcome of the exhibited work is applied to improve the productivity of the presented approach.

The above Figure 5 depicts the graphical representation of the comparative analysis made but the proposed 4G/5G OFDM and the OFF method. The parameter taken for the analysis is SNR and BER. From the analysis, the BER of the proposed method gradually decreases than the other existing technique.

The above Figure 6 depicts the graphical representation of the comparative analysis made but the proposed 4G/5G OFDM and the existing technique. The parameter taken for the analysis is SNR and downlink throughput (DLT). From the analysis, the DLT of the proposed method gradually increases when compared to the other existing technique.

The above Figure 7 illustrates the comparison of the proposed technique with multi-equalizer and MMSE. From the analysis results, the proposed method reduces the BER and error rate and improves the spectral efficiency, ULT, and DLT when compared to the other OFF techniques.

The above Figure 8 illustrates the comparison analysis of the proposed method with the multi-equalizer and MMSE in

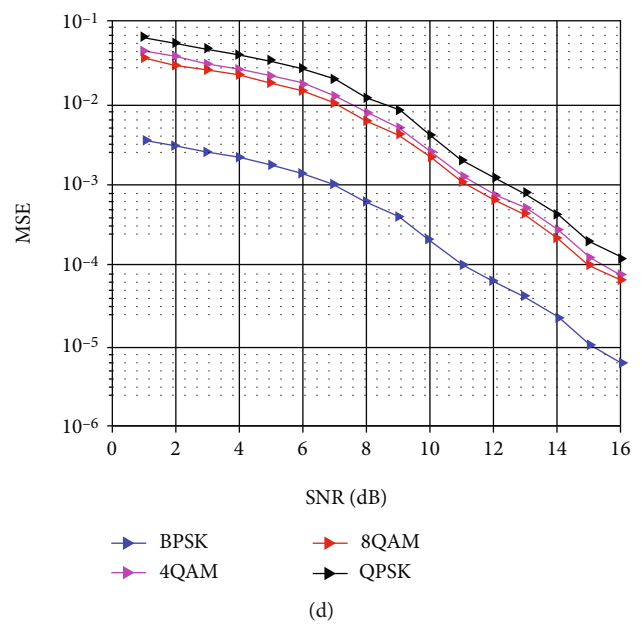
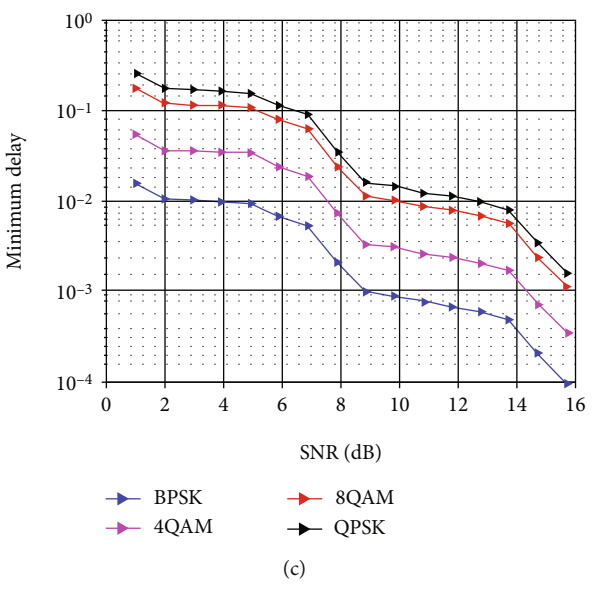
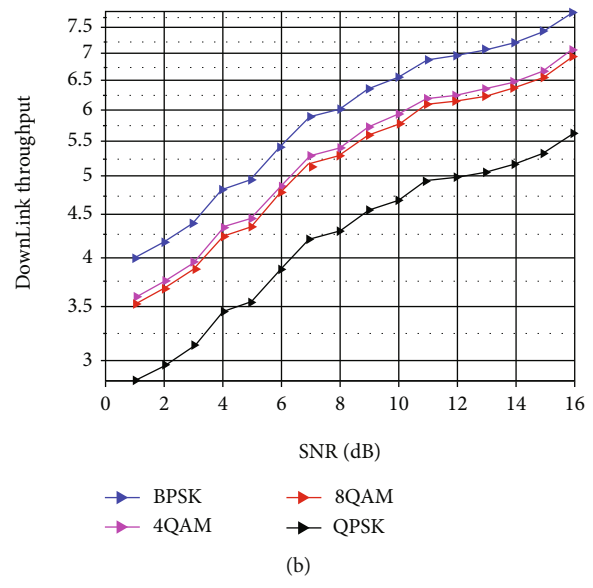
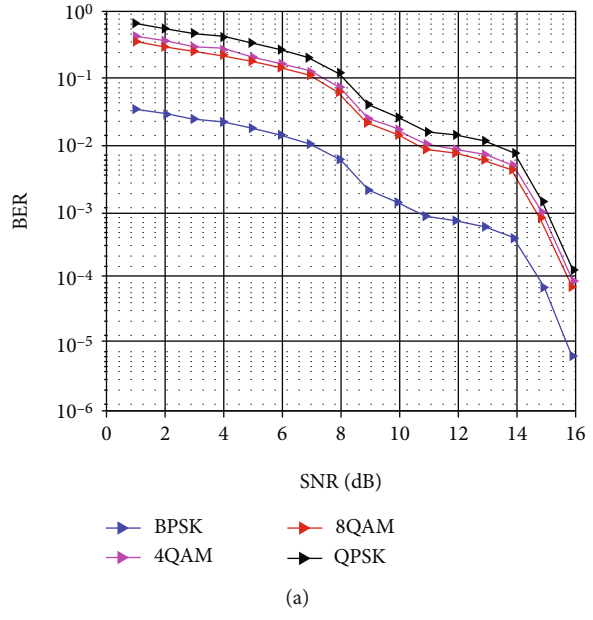


FIGURE 11: Continued.

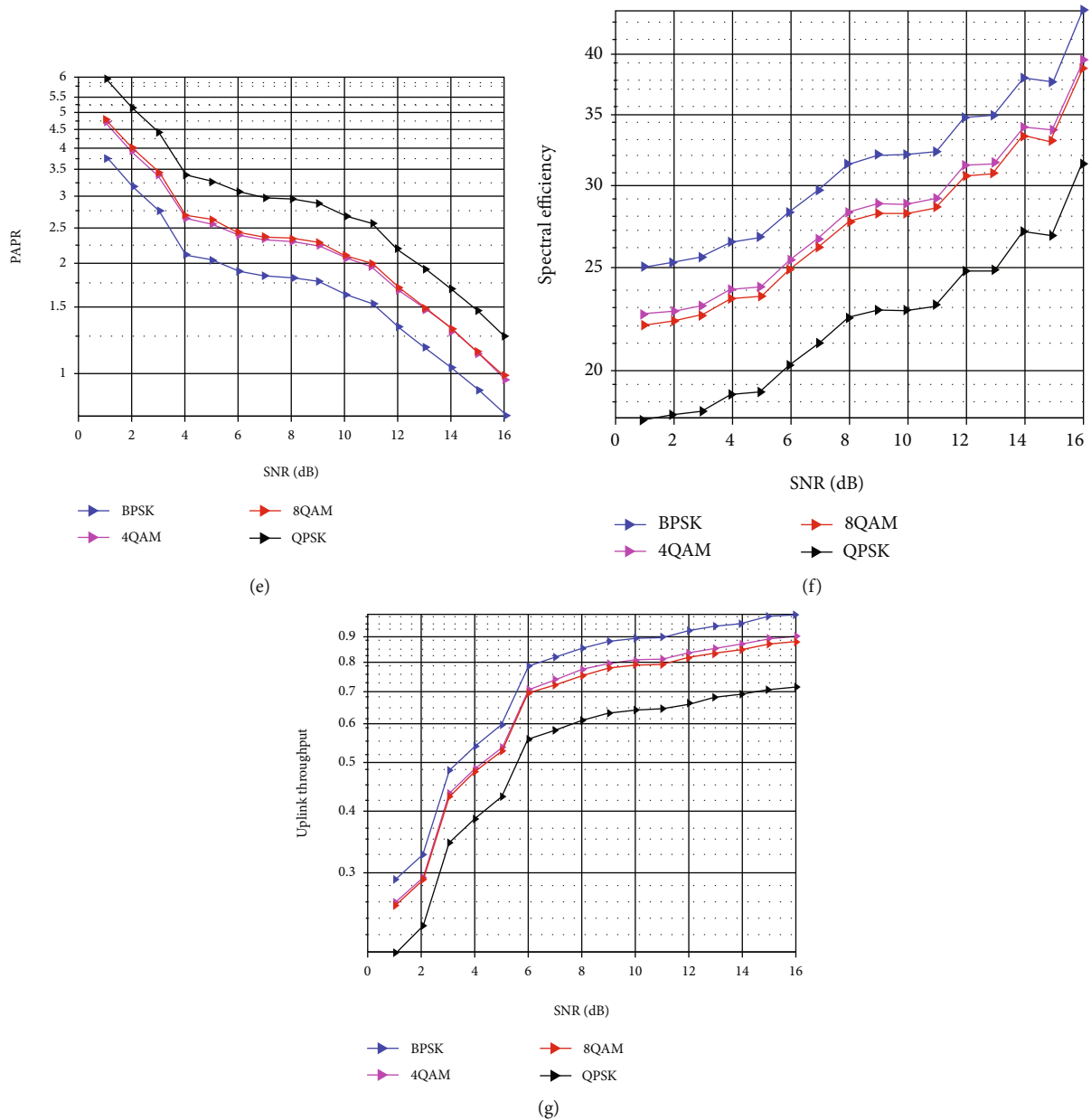


FIGURE 11: Comparative analysis depending on various modulators in terms of (a) BER, (b) DLT, (c) minimum delay, (d) MSE, (e) PAPR, (f) spectral efficiency, and (g) ULT.

terms of SNR-based spectral efficiency. As a result of the analysis, the spectral efficiency of the proposed methods is gradually increased when compared to the existing method.

The above Figure 9 illustrates the comparison of the proposed technique with the multi-equalizer and MMSE in terms of PAPR (Peak-Average Power Reduction). The analysis result shows that the proposed technique minimizes the delay when compared to the other existing technique.

The above Figure 10 illustrates the comparative analysis of the proposed method with multi-equalizer and MMSE. From the analysis results, the proposed method reduces the BER and error rate and improves the spectral efficiency, ULT, and DLT when compared to the other OFF techniques.

Figure 11 illustrates the comparative analysis of various modulators such as 4QAM, 8QAM, and QPSK with the BPSK in terms of BER, downlink as well as uplink throughput, minimum delay, spectral efficiency, MSE, and PAPR. The simulation results indicate that the proposed BPSK reduces the noise interference and error BER and provides an accurate decision than the other modulators.

### 5. Conclusion

This research work mainly focused on the reduction of the BER value of the OFDM model which relies on the LTE-based IoT. Here, the proposed framework encircles through the BPSK

when there occur contrasted with additional adjustment plots under AWGN (Additive White Gaussian Noise) channel. The performance of the DWT-OFDM through BPSK provides some specific unique properties which rely on other balance approaches. Therefore, BPSK is the most suitable application with low-speed communication. The input signals are simulated through various wavelets such as biorthogonal, Haar, Symlet, and Daubechies. The simulation is carried out through the MATLAB platform. The simulation results yield the optimal wavelet coefficient based on the plan which also provides the minimum average BER.

## Data Availability

The data used to support the findings of this study are included within the article. Should further data or information be required, these are available from the corresponding author upon request.

## Disclosure

It was performed as a part of the Employment of College.

## Conflicts of Interest

The authors declare that there are no conflicts of interest regarding the publication of this paper.

## Acknowledgments

The authors thank the Shree Institute of Technological Education, Tirupati for providing characterization supports to complete this research work.

## References

- [1] A. Hariri and M. Babaie-Zadeh, "Compressive detection of sparse signals in additive white Gaussian noise without signal reconstruction," *Signal Processing*, vol. 131, pp. 376–385, 2017.
- [2] L. Li and J. Wang, "Research on feature importance evaluation of wireless signal recognition based on decision tree algorithm in cognitive computing," *Cognitive Systems Research*, vol. 52, pp. 882–890, 2018.
- [3] T. Yucek and H. Arslan, "OFDM signal identification and transmission parameter estimation for cognitive radio applications," in *IEEE GLOBECOM 2007-IEEE Global Telecommunications Conference*, pp. 4056–4060, Washington, DC, USA, 2007, November.
- [4] R. Miyagusuku, A. Yamashita, and H. Asama, "Precise and accurate wireless signal strength mappings using Gaussian processes and path loss models," *Robotics and Autonomous Systems*, vol. 103, pp. 134–150, 2018.
- [5] W. Cao, W. Hu, L. Zhang, and J. Lei, "Pilots-aided LTE reference signal reconstruction in low SNR reference channel for passive sensing," in *2017 IEEE Asia Pacific Microwave Conference (APMC)*, pp. 97–100, Kuala Lumpur, Malaysia, 2017, November.
- [6] H. A. Akkar, W. A. Hadi, and I. H. Al-Dosari, "SA Squared-Chebyshev wavelet thresholding based 1D signal compression," *Defense Technology*, vol. 15, no. 3, pp. 426–431, 2019.
- [7] S. Alam and D. De, "Bio-inspired smog sensing model for wireless sensor networks based on intracellular signalling," *Information Fusion*, vol. 49, pp. 100–119, 2019.
- [8] R. K. Upadhyay and S. Kumari, "Detecting malicious chaotic signals in wireless sensor network," *Physica A: Statistical Mechanics and its Applications*, vol. 492, pp. 1129–1152, 2018.
- [9] L. Yunfei, L. Bing, Y. Yue, and M. Jidan, "Signal enhancement algorithm based on minimum mean square error spectrum estimation," in *2018 IEEE International Conference on Signal Processing, Communications and Computing (ICSPCC)*, pp. 1–4, Qingdao, China, 2018, September.
- [10] J. H. Bang, Y. J. Cho, and K. Kang, "Anomaly detection of network-initiated LTE signaling traffic in wireless sensor and actuator networks based on a Hidden semi-Markov Model," *Computers & Security*, vol. 65, pp. 108–120, 2017.
- [11] X. Yan, F. Long, J. Wang, N. Fu, W. Ou, and B. Liu, "Signal detection of the MIMO-OFDM system based on auto-encoder and extreme learning machine," in *2017 International Joint Conference on Neural Networks (IJCNN)*, pp. 1602–1606, Anchorage, AK, USA, 2017, May.
- [12] G. Zheng, Q. Gao, C. Gong, and Z. Xu, "Achievable rate and optimal signaling for an optical wireless decode-and-forward relaying channel," in *2016 IEEE Global Conference on Signal and Information Processing (GlobalSIP)*, pp. 16–19, Washington, DC, USA, 2016, December.
- [13] H. Meng and M. Sahin, "An electroacoustic recording device for wireless sensing of neural signals," in *2013 35th Annual International Conference of the IEEE Engineering in Medicine and Biology Society (EMBC)*, pp. 3086–3088, Osaka, 2013, July.
- [14] A. Bertrand, "Distributed signal processing for wireless EEG sensor networks," *IEEE Transactions on Neural Systems and Rehabilitation Engineering*, vol. 23, no. 6, pp. 923–935, 2015.
- [15] A. Hassani, J. Plata-Chaves, M. H. Bahari, M. Moonen, and A. Bertrand, "Multi-task wireless sensor network for joint distributed node-specific signal enhancement, LCMV beamforming, and DOA estimation," *IEEE Journal of Selected Topics in Signal Processing*, vol. 11, no. 3, pp. 518–533, 2017.
- [16] F. de la Hucha Arce, F. Rosas, M. Moonen, M. Verhelst, and A. Bertrand, "Generalized signal utility for LMMSE signal estimation with application to greedy quantization in wireless sensor networks," *IEEE Signal Processing Letters*, vol. 23, no. 9, pp. 1202–1206, 2016.
- [17] C. Chi and Z. Li, "Design of modulated excitation waveform based on OFDM signals for medical ultrasound imaging," in *2014 12th International Conference on Signal Processing (ICSP)*, pp. 102–107, Hangzhou, China, 2014, October.
- [18] S. Zheng and J. Kostamovaara, "The statistical behavior of a comparator with weak repetitive signal and additive white Gaussian noise," in *2016 IEEE International Instrumentation and Measurement Technology Conference Proceedings*, pp. 1–5, Taipei, Taiwan, 2016, May.
- [19] J. K. Hwang, C. F. Li, C. M. Chen, and Y. W. Pan, "Cost-effective software-defined radio approach to cross-platform LTE vector signal analysis," in *2016 IEEE Symposium on Computer Applications & Industrial Electronics (ISCAIE)*, pp. 7–10, Penang, Malaysia, 2016, May.
- [20] W. A. Jerjawi, Y. A. Eldemerdash, and O. A. Dobre, "Second-order cyclostationarity-based detection of LTE SC-FDMA signals for cognitive radio systems," *IEEE Transactions on Instrumentation and Measurement*, vol. 64, no. 3, pp. 823–833, 2014.

- [21] T. Anuradha, T. Lakshmi Surekha, P. Nuthakki, B. Domathoti, G. Ghorai, and F. A. Shami, "Graph theory algorithms of Hamiltonian cycle from quasi-spanning tree and domination based on vizing conjecture," *Journal of Mathematics*, vol. 2022, Article ID 1618498, 7 pages, 2022.
- [22] M. A. Bitew, R. K. Shiu, P. C. Peng, C. H. Wang, and Y. M. Chen, "Simultaneous transmission of wired and wireless signals based on double sideband carrier suppression," *Optical Fiber Technology*, vol. 38, pp. 108–112, 2017.
- [23] E. Karami, O. A. Dobre, and N. Adnani, "Identification of GSM and LTE signals using their second-order cyclostationarity," in *2015 IEEE International Instrumentation and Measurement Technology Conference (I2MTC) Proceedings*, pp. 1108–1112, Pisa, Italy, 2015, May.